Proceedings of the
44th IEEE Conference on Decision and Control, and
the European Control Conference 2005
Seville, Spain, December 12-15, 2005

A Modeling Framework for Six Degree-of-Freedom Control of Unmanned Sea Surface Vehicles

P. Krishnamurthy, F. Khorrami, S. Fujikawa

***Abstract*— A detailed six degree-of-freedom (DOF) nonlinear dynamic model of an Unmanned Sea Surface Vehicle (USSV) is developed. Models of the significant hydrodynamic effects including radiation-induced and damping forces and moments are incorporated. Disturbance models of forces and moments caused by ocean currents, waves, and wind are also included. Detailed models of the actuators including thrusters/propellers and control surfaces are included. To illustrate the importance of a six DOF modeling and the impact of disturbances, simulation results with two different controllers are presented. The detailed mathematical modeling in this paper is intended to provide the appropriate framework for a control design which explicitly addresses the six DOF USSV dynamics along with the disturbances.**

I. Introduction

We develop a detailed six DOF nonlinear dynamic model of a USSV. Models of the significant hydrodynamic effects including radiation-induced and damping forces and moments are incorporated. Disturbance models of forces and moments caused by ocean currents, waves, and wind are also included. Furthermore, detailed models of the actuators including thrusters/propellers and control surfaces are provided. While the models of each effect have long been available in the hydrodynamic literature [1–3], all the relevant effects have not been previously brought together in a synthesized setting that is tractable for use in a control design. Hence, control designs have so far been essentially based on a planar model [4–11] incorporating at most a highly simplified linearized model of the roll and pitch dynamics. The disturbances have also been so far treated as essentially exogenous noise inputs. However, as will be seen in the models derived in this paper, the actual forces and moments especially due to waves are highly coupled with the states. Hence, it is expected that controllers designed by explicitly addressing the disturbance models can achieve significantly better performance.

To illustrate the importance of a six DOF model and the impact of disturbances, simulation results with two different controllers are presented, one of the controllers being the controller of [11] which is based on tracking of a reference trajectory generated by a nominal planar subsystem and the other controller designed using a backstepping approach. It is seen that the backstepping-based controller which uses the yaw reference as an intermediate controller variable rather than an a priori provided reference trajectory performs better with incident waves. However, the backstepping-based controller is also based on the planar subsystem. It is expected that a controller that explicitly takes into account the form of the roll, pitch, and heave dynamics and the form of the disturbance forces and moments will be able to significantly out-perform the controllers derived based purely on the planar subsystem. Such a controller would be able to exploit the natural damping properties in the roll, pitch, and heave DOFs and model these DOFs as comprising the states of an appended Input-to-State Stable (ISS) dynamics. A crucial tool in the controller design would be the nonlinear small gain theorem [12]. The detailed mathematical modeling presented in this paper is intended to provide the appropriate framework for such a control design which explicitly addresses the six DOF dynamics of the USSV along with the disturbances.

The first two authors are with the Control/Robotics Research Laboratory (CRRL), Department of Electrical and Computer Engineering, Polytechnic University, Brooklyn, NY, 11201. The third author is with IntelliTech Microsystems, Inc., 17001 Science Dr., Suite 119, Bowie, MD 20715. This work was supported in part by ONR under contract No. N00014-04-M-0181. Emails: pk@crrl.poly.edu, khorrami@smart.poly.edu, sfujikawa@imicro.biz

II. Six DOF Kinematics and Dynamics of a USSV

In this section, we develop the rigid body kinematics and dynamics equations which govern the motion of the USSV. We will begin by developing the kinematic models of ship motion and then proceed to add the effects of mass and external torques to yield the dynamics equations.

Kinematics: Consider an inertial frame $X_iY_iZ_i$ with origin O_i and a body-fixed frame $X_bY_bZ_b$ with origin O_b. The rotation matrix R_i^b which transforms vectors in body-fixed frame to inertial frame can be parametrized in terms of three angles θ_x, θ_y, and θ_z as $R_i^b = R_{z,\theta_z}R_{y,\theta_y}R_{x,\theta_x}$ where R_{x,θ_x} denotes the rotation matrix corresponding to a rotation about X-axis by angle θ_x, etc. Hence,

$$R_i^b = \begin{bmatrix} c_yc_z & s_xs_yc_z - c_xs_z & c_xs_yc_z + s_xs_z \\ c_ys_z & s_xs_ys_z + c_xc_z & c_xs_ys_z - s_xc_z \\ -s_y & s_xc_y & c_xc_y \end{bmatrix} \quad (1)$$

where $c_x = \cos(\theta_x)$, $s_x = \sin(\theta_x)$, etc. The position and orientation of the ship relative to the inertial frame can be represented by $p = [p_t^T, p_r^T]^T$ where $p_t = [x, y, z]^T$ represents the coordinates of O_b as measured in the inertial frame and $p_r = [\theta_x, \theta_y, \theta_z]^T$ are the rotation angles. The translational and angular velocities of the ship relative to inertial frame and expressed in body-fixed frame are denoted as v_t and v_r, respectively. Let $v = [v_t^T, v_r^T]^T$. Hence,[1]

$$\dot{p}_t = R_i^b v_t = J_t(p_r)v_t \ ; \ J_t(p_r) = R_i^b. \quad (2)$$

$$\dot{R}_i^b = R_i^b S(v_r) \quad (3)$$

where $S(\omega)$ with $\omega = [\omega_x, \omega_y, \omega_z]^T$ denotes the skew-symmetric matrix $S(\omega) = \begin{bmatrix} 0 & -\omega_z & \omega_y \\ \omega_z & 0 & -\omega_x \\ -\omega_y & \omega_x & 0 \end{bmatrix}$. Denoting by e_1, e_2, and e_3 the three principal unit vectors, i.e., $e_1 = [1,0,0]^T$, $e_2 = [0,1,0]^T$, and $e_3 = [0,0,1]^T$, we have $\dot{R}_{x,\theta_x} = \dot{\theta}_x R_{x,\theta_x} S(e_1)$, $\dot{R}_{y,\theta_y} = \dot{\theta}_y R_{y,\theta_y} S(e_2)$, and $\dot{R}_{z,\theta_z} = \dot{\theta}_z R_{z,\theta_z} S(e_3)$. Hence,

$$\dot{R}_i^b = R_i^b S(\dot{\theta}_x e_1 + \dot{\theta}_y R_{x,\theta_x}^T e_2 + \dot{\theta}_z R_{x,\theta_x}^T R_{y,\theta_y}^T e_3). \quad (4)$$

Comparing with (3), v_r is related to $\dot{p}_r$ as

$$v_r = [e_1 \vdots R_{x,\theta_x}^T e_2 \vdots R_{x,\theta_x}^T R_{y,\theta_y}^T e_3]\dot{p}_r = \begin{bmatrix} 1 & 0 & -s_y \\ 0 & c_x & s_xc_y \\ 0 & -s_x & c_xc_y \end{bmatrix} \dot{p}_r \quad (5)$$

$$\dot{p}_r = J_r(p_r)v_r \ , \ J_r(p_r) = \begin{bmatrix} 1 & s_xt_y & c_xt_y \\ 0 & c_x & -s_x \\ 0 & s_x/c_y & c_x/c_y \end{bmatrix} \quad (6)$$

where $t_x = \tan(\theta_x)$ and $t_y = \tan(\theta_y)$. Using (2) and (6),

$$\dot{p} = J(p_r)v \ , \ J(p_r) = \begin{bmatrix} J_t(p_r) & 0_{3\times3} \\ 0_{3\times3} & J_r(p_r) \end{bmatrix}. \quad (7)$$

Dynamics: Denote by G the center of mass of the rigid body. Let $p_{G,i}$ and $p_{G,b}$ denote the coordinates of G relative to the inertial and body-fixed frames, respectively. Then, $p_{G,i} = p_t + R_i^b p_{G,b}$. Differentiating $p_{G,i}$ and using (2) and (3),

$$\dot{p}_{G,i} = R_i^b v_t + R_i^b S(v_r)p_{G,b} \quad (8)$$

$$\ddot{p}_{G,i} = R_i^b[\dot{v}_t + S(\dot{v}_r)p_{G,b}] + R_i^b S(v_r)[v_t + S(v_r)p_{G,b}]. \quad (9)$$

Denoting the mass of the ship by m and the net force acting on the ship expressed in body-fixed frame by F, the rigid body translational dynamics can be written as

$$m[\dot{v}_t + S(\dot{v}_r)p_{G,b} + S(v_r)v_t + S(v_r)S(v_r)p_{G,b} = F. \quad (10)$$

[1]Note that v_r is the angular velocity expressed in the body-fixed frame. The angular velocity in the inertial frame is $R_i^b v_r$. Hence, $\dot{R}_i^b = S(R_i^b v_r)R_i^b = R_i^b S(v_r)R_i^{bT}R_i^b = R_i^b S(v_r)$.

0-7803-9568-9/05/$20.00 ©2005 IEEE

Using the skew-symmetric matrix property that $S(a)b = a \times b = -b \times a = -S(b)a$, (10) can be rewritten as

$$m[\dot{v}_t - S(p_{G,b})\dot{v}_r + S(v_r)v_t - S(v_r)S(p_{G,b})v_r] = F. \quad (11)$$

Consider a decomposition of the rigid body into infinitesimal volume elements dV with local densities ρ_{dV}. Let $p_{dV,i}$ and $p_{dV,b}$ denote the coordinates of dV relative to the inertial and body-fixed frames, respectively, and let $v_{dV,i}$ denote the velocity of dV expressed in inertial frame. The net torque about O_b is given in the inertial frame by $\tau_i = \int [(p_{dV,i} - p_t) \times \dot{v}_{dV,i}]\rho_{dV} dV$ and in the body-fixed frame by

$$\begin{aligned} \tau &= R_i^{bT} \tau_i = R_i^{bT} \int [(p_{dV,i} - p_t) \times \dot{v}_{dV,i}]\rho_{dV} dV \\ &= \int \{p_{dV,b} \times [\dot{v}_t + S(\dot{v}_r)p_{dV,b} + S(v_r)v_t \\ &\quad + S(v_r)S(v_r)p_{dV,b}]\}\rho_{dV} dV. \end{aligned} \quad (12)$$

The mass m and the moment of inertia I_b (about the point O_b) satisfy, by definition, $mp_{G,b} = \int p_{dV,b}\rho_{dV} dV$, $I_b\dot{v}_r = \int \{p_{dV,b} \times [S(\dot{v}_r)p_{dV,b}]\}\rho_{dV} dV$, and $I_b = -\int S(p_{dV,b})S(p_{dV,b})\rho_{dV} dV$. Note that I_b is a constant symmetric positive-definite matrix. Using the vector triple product identity, we obtain $p_{dV,b} \times [S(v_r)S(v_r)p_{dV,b}] = -S(v_r)S(p_{dV,b})S(p_{dV,b})v_r$ so that $\int \{p_{dV,b} \times [S(v_r)S(v_r)p_{dV,b}]\}\rho_{dV} dV = S(v_r)I_b v_r = -S(I_b v_r)v_r$. Hence, (12) reduces to

$$\tau = mS(p_{G,b})\dot{v}_t + I_b\dot{v}_r + mS(p_{G,b})S(v_r)v_t - S(I_b v_r)v_r. \quad (13)$$

The rigid body kinematics (7) and the translational and rotational dynamics (11) and (13) can be rewritten as

$$\dot{p} = J(p)v \;\; ; \;\; M_{RB}\dot{v} + C_{RB}(v)v = \overline{F} \quad (14)$$

$$M_{RB} = \begin{bmatrix} mI_{3\times 3} & -mS(p_{G,b}) \\ mS(p_{G,b}) & I_b \end{bmatrix} \quad (15)$$

$$C_{RB}(v) = \begin{bmatrix} mS(v_r) & -mS(v_r)S(p_{G,b}) \\ mS(p_{G,b})S(v_r) & -S(I_b v_r) \end{bmatrix} \quad (16)$$

where $\overline{F}$ is the 6×1 generalized force vector given by $\overline{F} = [F^T, \tau^T]^T$. Note that M_{RB} is a constant symmetric positive-definite matrix while $C_{RB}(v)$ is a skew-symmetric matrix that depends on the angular velocity of the rigid body.

III. External Forces and Torques

The external forces and torques acting on a USSV consist of the following components:

1) *Hydrodynamic $\overline{F}_H$:* Radiation-induced and damping forces and moments caused due to gravity and the hydrodynamic resistance of the surrounding fluid.
2) *Environmental disturbances $\overline{F}_E$:* forces and moments caused by ocean currents, waves, and wind. These include Froude-Kriloff and diffraction forces caused by incident waves.
3) *Propulsion $\overline{F}_P$:* forces and moments due to actuators (thrusters/propellers, control surfaces, rudders, fins).

The radiation-induced forces and moments $\overline{F}_R$ can be decomposed into three sub-components: (1) Added mass due to the inertia of the surrounding liquid = $-M_A\dot{v} - C_A(v)v$, (2) Radiation-induced potential damping due to energy carried away by generated surface waves = $-D_P(v)v$, and (3) Restoring forces due to Archimedean effects (weight and buoyancy) = $-g(p)$. The damping forces and moments $\overline{F}_D$ can also be decomposed into three sub-components: (1) Skin friction = $-D_S(v)v$, (2) Wave drift damping = $-D_W(v)v$, and (3) Vortex shedding damping = $-D_M(v)v$. Hence,

$$\overline{F}_H = \overline{F}_R + \overline{F}_D = -M_A\dot{v} - C_A(v)v - D_H(v)v - g(p) \quad (17)$$

$$D_H(v) = D_P(v) + D_S(v) + D_W(v) + D_M(v). \quad (18)$$

Using (14), the dynamics of the vehicle can be written as

$$\dot{p} = J(p)v \;\; ; \;\; M_H\dot{v} + C_H(v)v + D_H(v)v + g(p) = \overline{F}_E + \overline{F}_P \quad (19)$$

where $M_H = M_{RB} + M_A$ and $C_H(v) = C_{RB}(v) + C_A(v)$. The various external forces and moments are treated in greater detail in the following subsections.

A. Hydrodynamic Forces and Moments

Added Mass: The generalized force vector due to added mass effects is of the form $-M_A\dot{v} - C_A(v)v$. The matrix M_A can be shown to be symmetric and positive-definite if the rigid body is completely submerged or if the rigid body is almost at rest ($v \approx 0$). However, for fast-moving surface ships, M_A is non-symmetric. C_A is a skew-symmetric matrix. For slender bodies, an approximate estimate for M_A can be obtained by applying strip theory which entails dividing the submerged part of the ship into a number of strips, computing two-dimensional hydrodynamic coefficients for added mass for each strip, and integrating over the length of the ship to obtain the three-dimensional coefficients. The matrix C_A is obtained from M_A as

$$C_A(v) = \begin{bmatrix} 0_{3\times 3} & -S(M_{A,11}v_t + M_{A,12}v_r) \\ -S(M_{A,11}v_t + M_{A,12}v_r) & -S(M_{A,21}v_t + M_{A,22}v_r) \end{bmatrix}$$

where $M_{A,ij}$ denotes the $(i,j)^{th}$ 3×3 submatrix of M_A.

Hydrodynamic Damping: The hydrodynamic forces and moments are primarily generated by four effects, namely radiation-induced potential damping ($-D_P(v)v$), skin friction ($-D_S(v)v$), wave drift damping ($-D_W(v)v$), and vortex shedding ($-D_M(v)v$). The total hydrodynamic damping matrix $D_H(v)$ is therefore given by (18). The dissipativity of hydrodynamic damping forces implies that $D_H(v)$ is a strictly positive matrix. Radiation-induced potential damping is caused due to forces on the ship when the ship is forced to oscillate with the wave excitation frequency in the absence of incident waves. Potential damping terms may be significant for surface vehicles but are usually negligible for underwater vehicles. Skin friction is caused due to effects at the boundary layer. Linear skin friction due to laminar boundary effects is significant during low-frequency motion of the vehicle. At high frequencies, a nonlinear (mainly quadratic) skin friction term is caused due to boundary layer turbulence. Wave drift damping which is caused due to added resistance for surface vehicles advancing in waves is proportional to the square of the significant wave height and is therefore the predominant damping contribution to surge for higher sea states. Damping due to vortex shedding which is caused by viscous damping forces on a ship moving through a viscous fluid depends on the kinematic viscosity coefficient of the fluid.

Restoring Forces: The gravitational and buoyancy forces are referred to, in hydrodynamic terminology, as restoring forces. Taking the z-axis to be pointing upwards, the gravitational force f_G and the buoyancy force f_B are given by

$$f_G(p) = R_i^{bT}[0, 0, -mg]^T, \; f_B(p) = R_i^{bT}[0, 0, \rho g \nabla(p)]^T \quad (20)$$

where g is the acceleration due to gravity, ρ is the density of water, and $\nabla(p)$ is the displaced volume of water when the vehicle is in the configuration p. The gravitational force acts through the center of gravity G while the buoyancy force acts through the center of buoyancy B. Denoting the coordinates of G and B in the body-fixed frame by $p_{G,b}$ and $p_{B,b}$, the generalized force vector due to restoring effects is given by

$$g(p) = -\begin{bmatrix} f_G(p) + f_B(p) \\ p_{G,b} \times f_G(p) + p_{B,b} \times f_B(p) \end{bmatrix}. \quad (21)$$

The displaced volume $\nabla(p)$ is constant for underwater vehicles. However, in the case of surface vehicles, $\nabla(p)$ is a complicated function of the detailed vehicle geometry. Taking $z = 0$ to be the nominal submersion of the ship, i.e., $m = \rho\nabla([0, \ldots, 0]^T)$, considerable simplification can be achieved for small rotations using the practically meaningful assumptions of symmetry about xz (left-right) and yz (front-back) planes yielding

$$\begin{aligned} g(p) &\approx \rho g \mathrm{diag}(R_i^{bT}, R_i^{bT}) \\ &\quad \times [0, 0, A_{wp}z, \nabla\overline{GM_T}\sin(\theta_x), \nabla\overline{GM_L}\sin(\theta_y), 0]^T \end{aligned} \quad (22)$$

where $\nabla = m/\rho$ is the nominal displaced volume of water, A_{wp} is the water plane area (area of the vehicle crosssection at the water surface), and $\overline{GM_T}$ and $\overline{GM_L}$ denote the transverse and longitudinal metacentric heights, respectively. The transverse metacenter M_T and the longitudinal metacenter M_L lie on the line

BG (the *keel line*). The transverse and longitudinal metacentric heights are defined through the relations $\overline{GM_T} = \overline{BM_T} - \overline{BG}$, $\overline{BM_T} = I_T/\nabla$, $I_T = \int\int_{A_{wp}} y^2 dA$, $\overline{GM_L} = \overline{BM_L} - \overline{BG}$, $\overline{BM_L} = I_L/\nabla$, and $I_L = \int\int_{A_{wp}} x^2 dA$. If $\overline{GM_T}$ and $\overline{GM_L}$ are positive (*metacentric stability*), the restoring forces (22) tend to stabilize (i.e., oppose roll, pitch, and heave) the vehicle.

B. Environmental Disturbances

The generalized force vector due to environmental disturbances is the sum of three components: $\overline{F}_E = \overline{F}_{\text{current}} + \overline{F}_{\text{wave}} + \overline{F}_{\text{wind}}$ caused due to the ocean currents, waves, and wind, respectively.

Ocean Currents: The forces and moments induced by ocean currents are of the form[2]

$$\overline{F}_{\text{current}} = \underbrace{M_{FK}\dot{V}_c}_{\text{Froude-Kriloff}} + \underbrace{M_A\dot{V}_c + D_P(V_c)V_c}_{\text{diffraction forces}} + \underbrace{(D_S(V_c) + D_W(V_c) + D_M(V_c))V_c}_{\text{viscous forces}} \quad (23)$$

where V_c is the fluid velocity vector expressed in the body-fixed frame. The Froude-Kriloff inertia matrix M_{FK} is the inertia matrix of the displaced fluid. If the vehicle is neutrally buoyant and the mass is homogeneously distributed, $M_{FK} = M_{RB}$ and for slowly-varying currents, the vehicle dynamics can be approximated by

$$M_H\dot{v}_r + C_H(v_r)v_r + D_H(v_r)v_r + g(p) = \overline{F}_{\text{wave}} + \overline{F}_{\text{wind}} + \overline{F}_P$$

where $v_r = v - V_c$ is the relative velocity. The position kinematics can be written as $\dot{p} = J(p)v_r + J(p)V_c = J(p)v_r + V_{c,i}$ where $V_{c,i}$ is the ocean current velocity expressed in inertial frame. For surface vehicles, $V_{c,i}$ can be adequately represented in terms of its magnitude and heading which can be modeled as random walks. The ocean current velocity magnitude V_c can be decomposed as $V_c = V_t + V_{lw} + V_s + V_m + V_{\text{set-up}} + V_d$ where V_t is the tidal component, V_{lw} is the component generated by local wind, V_s is the component generated by nonlinear waves (Stokes drift), V_m is the component caused by major ocean circulation (e.g., Gulf stream), $V_{\text{set-up}}$ is the component due to set-up phenomena and storm surges, and V_d is the local density driven current components governed by strong density jumps in the upper ocean. Velocity profile of the tidal component V_t can be modeled as a function of depth as $V_t(z) = V_t(0)$ for $0 \geq z \geq 10 - d$ and $V_t(z) = V_t(0)\log_{10}\left(1 - \frac{9z}{d-10}\right)$ for $10 - d > z > -d$ where $V_t(0)$ is the surface velocity of the tidal component and $d > 10$ is the water depth. The component generated by local wind can be modeled as $V_{lw}(z) = V_{lw}(0)\frac{d_0+z}{d_0}$ for $0 \geq z \geq -d_0$ and $V_{lw}(z) = 0$ for $-d_0 > z$ where $d_0(\approx 50\text{m})$ is the reference depth for the wind-generated current and $V_{lw}(0)$ is approximately $0.02V_{10}$ with V_{10} being the wind velocity measured 10m above sea level. The Stokes drift which results from the irrotational properties of the waves can be modeled as $V_s(z) = \sum_{i=1}^{N} \frac{2\pi\omega_i A_i^2}{\lambda_i} \exp\left(\frac{4\pi z}{\lambda_i}\right)$ where A_i, ω_i, and λ_i are the amplitude, frequency, and wavelength, respectively, of the i^{th} wave component, $i = 1, \ldots, N$, with N being the number of wave components.

Waves: The incident waves and the resulting forces and moments on the ship can be characterized in terms of the velocity potential [1]. For ideal fluids (no shear stresses) under irrotational flow ($\nabla \times V = 0$ where V is the fluid velocity), the velocity $V(x, y, z, t)$ can be expressed as the gradient of a scalar velocity potential $\phi(x, y, z, t)$, i.e., $V = \nabla\phi$. Conservation of mass yields the *Laplace's equation* $\nabla^2\phi = 0$. To obtain ϕ, Laplace's equation must be solved under appropriate boundary conditions. A kinematic boundary condition which must be imposed on any boundary surface with a specified geometry and position (e.g., a ship hull) is that the normal components of the boundary velocity and the fluid velocity at the boundary must be equal. If the boundary surface is not known (e.g., the free surface of the water in contact with air), the kinematic boundary condition can not be directly used. Instead, a dynamic boundary condition which specifies that the pressure at the free surface is equal to the atmospheric pressure is utilized. By Bernoulli's equation (which is derived from the conservation of linear momentum), the dynamic pressure $p_{\text{dyn}}(x, y, z, t)$ is given in terms of the velocity potential as

$$p_{\text{dyn}}(x, y, z, t) = -\rho[\frac{\partial\phi}{\partial t} + \frac{1}{2}\nabla\phi.\nabla\phi] \quad (24)$$

where ρ is the fluid density. The total pressure $p(x, y, z, t)$ is given by the sum of the dynamic pressure $p_{\text{dyn}}(x, y, z, t)$ and the hydrostatic pressure $(p_a - \rho g z)$ (taking $z = 0$ to denote the nominal free surface in the absence of waves) where p_a is the atmospheric pressure. The wave solutions can be obtained as solutions of Laplace's equation under suitable boundary conditions at the free surface. Let the elevation of the wave be denoted by $\zeta(x, y, t)$, i.e., the two-dimensional surface $z = \zeta(x, y, t)$ provides the free surface in contact with the air at time t. The kinematic boundary condition is given by $\frac{D}{Dt}(z - \zeta) = 0$ on the surface $z = \zeta(x, y, t)$ where $\frac{D}{Dt} \triangleq \frac{\partial}{\partial t} + V.\nabla$ denotes the substantial (or total) derivative. The dynamic boundary condition is given by

$$\left\{-\rho\left[\frac{\partial\phi}{\partial t} + \frac{1}{2}\nabla\phi.\nabla\phi\right] + p_a - \rho g z\right\}_{z=\zeta} = p_a. \quad (25)$$

The constant p_a on both sides of the equation (25) cancels out and can be neglected in all ensuing derivations of forces and moments caused by incident waves. This corresponds to the fact that a constant pressure influences only the hydrostatic restoring force (buoyancy). Eliminating ζ between the kinematic boundary condition and the dynamic boundary condition (25) yields

$$\left\{\frac{D}{Dt}\left(z + \frac{1}{g}\left[\frac{\partial\phi}{\partial t} + \frac{1}{2}\nabla\phi.\nabla\phi\right]\right)\right\}_{z=\zeta} = 0 \quad (26)$$

$$\implies g\frac{\partial\phi}{\partial z} + \frac{\partial^2\phi}{\partial t^2} + 2\nabla\phi.\nabla\frac{\partial\phi}{\partial t} + \frac{1}{2}\nabla\phi.\nabla(\nabla\phi.\nabla\phi) = 0 \quad (27)$$

valid on the free surface $z = \zeta(x, y, t)$. In the case of finite depth of the sea floor, an additional boundary condition must be imposed at the sea floor. Assuming that the sea floor is flat and at depth H, i.e., the sea floor is given by the surface $z = -H$, the condition that the normal velocity at the sea floor is zero is given by $\frac{\partial\phi}{\partial z}\big|_{z=-H} = 0$. If the sea is assumed to be of infinite depth, the finite-depth boundary condition can be replaced by the requirement that $\phi \to 0$ as $z \to -\infty$. The results under infinite depth assumption can also be obtained by taking the limit of the solution in the finite depth case as $H \to \infty$. Upon computing the velocity potential $\phi(x, y, z, t)$ of the wave, the dynamic pressure distribution is given by (24) and the wave-induced generalized force vector on a rigid body with surface S_B in contact with the water is given by

$$\overline{F}_{\text{wave}} = \begin{bmatrix} -\rho\int\int_{S_B}[\frac{\partial\phi}{\partial t} + \frac{1}{2}\nabla\phi.\nabla\phi]n dS \\ -\rho\int\int_{S_B}[\frac{\partial\phi}{\partial t} + \frac{1}{2}\nabla\phi.\nabla\phi](r \times n)dS \end{bmatrix} \quad (28)$$

where n is the unit normal to the ship surface pointing into the ship. The quadratic term $\nabla\phi.\nabla\phi$ in the integrand in (28) is often neglected making $\overline{F}_{\text{wave}}$ proportional to ϕ. This yields the principle of superposition whereby different hydrodynamic and hydrostatic effects can be considered separately and resulting generalized force vectors added to obtain the total forces and moments. When a ship encounters an incident wave, three effects are involved. Firstly, the ship experiences forces (and moments) as a direct result of the incident waves. These forces would be the same even if the ship is constrained so that it can not move. These forces are investigated in greater detail in the rest of this section. Secondly, the motion of the ship under the action of the original incident waves excites the surrounding fluid and causes new waves. The forces on the ship (*radiation-induced potential damping*) caused by interaction with the new waves were considered in the discussion on damping forces above. Thirdly, the incident waves undergo a scattering and dispersion effect due to the presence of the ship. This is known as *wave drift damping* and was treated before. By superposition, these three effects can be considered independently. The first effect which is the direct action of the incident wave on the rigid body is usually the most significant, especially for slender ships.

[2]For notational clarity, fluid velocities are denoted as V while the lower case v is reserved for rigid body velocities.

Using Taylor series expansions of the form $\phi(x,y,\zeta,t) = \phi(x,y,0,t) + \zeta\left(\frac{\partial\phi}{\partial z}\right)_{z=0} + \frac{1}{2}\zeta^2\left(\frac{\partial^2\phi}{\partial z^2}\right)_{z=0} + \ldots$, the boundary condition (27) which is prescribed on the unknown free surface $z = \zeta(x,y,t)$ can be replaced by a sequence of boundary conditions on $z = 0$, the first two members of the sequence being

$$\frac{\partial^2\phi}{\partial t^2} + g\frac{\partial\phi}{\partial z} = 0 \quad (29)$$

$$\frac{\partial^2\phi}{\partial t^2} + g\frac{\partial\phi}{\partial z} + 2\nabla\phi.\nabla\frac{\partial\phi}{\partial t} - \frac{1}{g}\frac{\partial\phi}{\partial t}\frac{\partial}{\partial z}\left(\frac{\partial^2\phi}{\partial t^2} + g\frac{\partial\phi}{\partial z}\right) = 0. \quad (30)$$

The solutions to the first-order problem, i.e., Laplace's equation under the finite-depth boundary condition and (29), are given in closed form as

$$\begin{aligned}\phi(x,y,z,t) &= \frac{gA}{\omega}\frac{\cosh(k[z+H])}{\cosh(kH)} \\ &\quad \times \sin(kx\cos(\theta_{\text{wave}}) + ky\sin(\theta_{\text{wave}}) - \omega t) \quad (31)\end{aligned}$$

where k, ω, A, and θ_{wave} are real numbers with k and ω satisfying the dispersion relation $k\tanh(kH) = \omega^2/g$. Any linear combination of functions of the form (31) is also a solution to the first-order problem. Physically, k is the wave number (wavelength $\lambda = 2\pi/k$), ω is the frequency (period $T = 2\pi/\omega$), A is the wave amplitude, and θ_{wave} gives the direction of propagation of the wave. The dispersion relation links the wave number and the frequency and is derived from the finite-depth boundary condition. Since ω is not proportional to k, the phase velocity $V_p = \omega/k = \sqrt{(g/k)\tanh(kH)}$ depends on the wave number. Hence, water wave propagation is dispersive with longer waves traveling faster than shorter waves. Two special cases of practical interest are the deep water case ($H = \infty$) and the shallow water case ($H \approx 0$). In the deep water case, the dispersion relation reduces to $k = \omega^2/g$ so that the phase velocity $V_p = \sqrt{\frac{g\lambda}{2\pi}}$ is proportional to the square root of the wavelength. In the shallow water case, the dispersion relation simplifies to $k^2H = \omega^2/g$ so that the phase velocity $V_p = \sqrt{gH}$ is constant. Hence, wave motion in shallow water is nondispersive. From the solution (31) to the first-order problem, elevation of the free water surface $\zeta(x,y,t) = -\frac{1}{g}\frac{\partial\phi}{\partial t}\big|_{z=0}$ is

$$\zeta(x,y,t) = A\cos(kx\cos(\theta_{\text{wave}}) + ky\sin(\theta_{\text{wave}}) - \omega t) \quad (32)$$

Also, the fluid velocity $V(x,y,z,t)$ can be obtained as $V(x,y,z,t) = \nabla\phi$. In the deep-water limit, (31) reduces to

$$\phi = \frac{gA}{\omega}e^{kz}\sin(kx\cos(\theta_{\text{wave}}) + ky\sin(\theta_{\text{wave}}) - \omega t) \quad (33)$$

which, as can be verified by direct substitution, also satisfies the second-order boundary condition (30). Hence, in the deep-water case, (33) is also a solution to the second-order problem. The elevation $\zeta(x,y,t)$ can be computed using the solution (33) to the second-order problem in the deep-water case to be

$$\begin{aligned}\zeta(x,y,t) &= -\frac{1}{g}\left[\frac{\partial\phi}{\partial t} + \frac{1}{2}\nabla\phi.\nabla\phi - \frac{1}{g}\frac{\partial\phi}{\partial t}\frac{\partial^2\phi}{\partial z\partial t}\right]_{z=0} \\ &= A\cos(kx\cos(\theta_{\text{wave}}) + ky\sin(\theta_{\text{wave}}) - \omega t) \\ &\quad + \frac{1}{2}A^2k\cos(2kx\cos(\theta_{\text{wave}}) + 2ky\sin(\theta_{\text{wave}}) - 2\omega t) \quad (34)\end{aligned}$$

Also, the fluid velocity can be computed using $V(x,y,z,t) = \nabla\phi$. It can be shown that (33) is also a solution to the third-order problem if the dispersion relation is modified to $\omega^2 = gk(1+k^2A^2)$ from which the phase velocity is obtained as $V_p = \frac{\omega}{k} = \sqrt{\frac{g}{k}(1+k^2A^2)}$ implying that longer waves travel faster than shorter waves and taller waves travel faster than waves of smaller height.

Using the family of solutions (32), the general solution to the first-order problem in the deep-water case with continuous spectral and directional content of the wave can be written as the Fourier-Stieltges integral $\zeta(x,y,t) = \int\int dA(\omega,\theta_{\text{wave}})\cos[kx\cos(\theta_{\text{wave}}) + ky\sin(\theta_{\text{wave}}) - \omega t + \phi_{\text{wave}}(\omega,\theta_{\text{wave}})]$ where $k = \omega^2/g$ as given by the deep-water dispersion relation. The random wave pattern in an irregular sea can be modeled with the component phases ϕ_{wave} being (uniformly distributed) random variables and the amplitudes $dA(\omega,\theta_{\text{wave}})$ being determined by an energy spectrum. The average energy density, i.e., the average value of $\zeta(x,y,t)$ is given by $\overline{\zeta^2} = \frac{1}{2}\int\int dAdA^* \triangleq \int_0^\infty\int_0^{2\pi}S(\omega,\theta_{\text{wave}})d\theta_{\text{wave}}d\omega$ where the *directional energy spectrum* $S(\omega,\theta_{\text{wave}})$ is the energy density in the differential element of the frequency-direction space bounded by $(\omega,\omega+d\omega)$ and $(\theta_{\text{wave}},\theta_{\text{wave}}+d\theta_{\text{wave}})$. Hence, the magnitude of the differential wave amplitude is proportional to the square root of the total energy in the differential element of the frequency-direction space bounded by $(\omega,\omega+d\omega)$ and $(\theta_{\text{wave}},\theta_{\text{wave}}+d\theta_{\text{wave}})$. $S(\omega,\theta_{\text{wave}})$ can also be interpreted as the Fourier transform of the correlation function for the free surface elevation. It can be shown that the total mean energy of the wave system per unit area of the free surface is equal to $\rho g\int_0^\infty\int_0^{2\pi}S(\omega,\theta_{\text{wave}})d\theta_{\text{wave}}d\omega$. Integrating over all wave directions, the *frequency spectrum* or the *wave spectral density function* is obtained as $S(\omega) = \int_0^{2\pi}S(\omega,\theta_{\text{wave}})d\theta_{\text{wave}}$. A commonly used model for $S(\omega)$ based on empirical observations for a fully-developed sea is the Pierson-Moskowitz (PM) spectrum $S(\omega) = \frac{\alpha g^2}{\omega^5}\exp\left(-\beta\left[\frac{g}{V_{19.5}\omega}\right]^4\right)$ where $\alpha = 8.1\times10^{-3}$, $\beta = 0.74$, and $V_{19.5}$ is the wind velocity at 19.5 m above the free surface.

When viewed relative to the body-fixed frame, the apparent frequency (*encounter frequency*) of a wave component is given by $\omega_e = \omega - k\dot{x}\cos(\theta_{\text{wave}}) - k\dot{y}\sin(\theta_{\text{wave}})$. Denoting $v_{\text{ship}} = \sqrt{\dot{x}^2+\dot{y}^2}$ and $\theta_{\text{ship}} = \text{atan}(\dot{y}/\dot{x})$ and using the dispersion relation $k = \omega^2/g$, we obtain $\omega_e = \omega - \frac{\omega^2}{g}v_{\text{ship}}\cos(\theta_{\text{wave}} - \theta_{\text{ship}})$. Thus, when $v_{\text{ship}} \neq 0$, two different frequencies ω in the inertial frame map to each frequency ω_e as seen in the moving frame.

Wind: As in the treatment of waves, the forces and moments caused by wind can be obtained by integrating a pressure distribution over the ship surface exposed to air. However, setting up boundary problems for wind is usually infeasible and wind gusts are usually beyond the controller frequency range. Hence, only the contribution due to average wind is modeled. Moreover, the average wind can be taken to be acting in the plane parallel to the nominal sea surface $z = 0$. Let the average wind velocity be $[V_{\text{wind}}\cos(\theta_{\text{wind}}), V_{\text{wind}}\sin(\theta_{\text{wind}}), 0]^T$. Then, the relative velocity of the average wind with respect to the ship has magnitude $V_{\text{wind,R}} = [(\dot{x} - V_{\text{wind}}\cos(\theta_{\text{wind}}))^2 + (\dot{y} - V_{\text{wind}}\sin(\theta_{\text{wind}}))^2]^{\frac{1}{2}}$ and direction $\theta_{\text{wind,R}} = \theta_{\text{wind}} - \theta_z$. The average wind primarily contributes to forces in the surge, sway, and yaw DOFs and the contribution is proportional to the square of the relative velocity. The contributions to surge and sway are proportional to the transverse projected area A_T and the lateral projected area A_L, respectively. The contribution to yaw is proportional to the product of the overall length L and the lateral projected area A_L. Hence, the generalized force vector due to average wind is given in inertial frame by $\overline{F}_{\text{wind,i}} = [\overline{F}_{\text{wind,X}}\cos(\theta_z) - \overline{F}_{\text{wind,Y}}\sin(\theta_z), \overline{F}_{\text{wind,X}}\sin(\theta_z) + \overline{F}_{\text{wind,Y}}\cos(\theta_z), 0, 0, 0, c_{\text{wind,3}}V_{\text{wind,R}}^2A_LL\sin(2\theta_{\text{wind,R}})]^T$ and in body-fixed frame by $\overline{F}_{\text{wind}} = \text{diag}(R_i^{b^T}, R_i^{b^T})\overline{F}_{\text{wind,i}}$ where $c_{\text{wind,1}}$, $c_{\text{wind,2}}$, and $c_{\text{wind,3}}$ are constants, $\overline{F}_{\text{wind,X}} = c_{\text{wind,1}}V_{\text{wind,R}}^2A_T\cos(\theta_{\text{wind,R}})$ and $\overline{F}_{\text{wind,Y}} = c_{\text{wind,2}}V_{\text{wind,R}}^2A_L\sin(\theta_{\text{wind,R}})$.

C. Propulsion

Thruster/Propeller: Propellers can be classified into fixed-pitch and controllable-pitch propellers (in which the propeller blades can be turned using a hydraulic servo). If the propeller axial direction expressed in body-fixed frame is a_{prop} (which is variable for a gimbaled propeller), the generalized force vector due to the propeller is $[T_{\text{prop}}a_{\text{prop}}, T_{\text{prop}}(r_{\text{prop}}\times a_{\text{prop}})]^T$ where r_{prop} is propeller position in body-fixed frame. The generalized force vector due to multiple propellers can be obtained by adding individual propeller contributions. The *advance coefficient* J_0 is defined as

$J_0 = v_{\text{prop}}/(n_{\text{prop}} D_{\text{prop}})$ where n_{prop} is rotational speed (in revs/sec), D_{prop} is propeller diameter, and the *advance speed* $v_{\text{prop}} = v_{\text{f,ship}}(1-w)$ is the incoming water speed with $v_{\text{f,ship}}$ being the ship forward speed relative to water in the propeller axial direction and w the *wake fraction* ($\sim$ 0.1-0.4). The propeller thrust T_{prop} and the propeller torque Q_{prop} are given by $T_{\text{prop}} = K_T \rho |n_{\text{prop}}| n_{\text{prop}} D_{\text{prop}}^4$ and $Q_{\text{prop}} = K_Q \rho |n_{\text{prop}}| n_{\text{prop}} D_{\text{prop}}^5$. The *thrust coefficient* K_T and the *torque coefficient* K_Q are approximately linear functions of J_0 given by $K_T = \alpha_1 - \alpha_2 J_0$ and $K_Q = \beta_1 - \beta_2 J_0$ with α_1, α_2, β_1, and β_2 being (usually) positive constants. For controllable-pitch propellers, α_1, β_1, and β_2 can be taken to be linear in propeller blade pitch with α_1 and β_2 approximately zero at zero pitch and α_2 independent of pitch. The propeller is coupled to the engine through a gear train. The engine rotational speed n_{engine} and the load torque on the engine Q_{load} are given by $n_{\text{engine}} = \lambda_{\text{gear}} n_{\text{prop}}$ and $Q_{\text{load}} = Q_{\text{prop}}/(\eta_{\text{gear}} \lambda_{\text{gear}})$ where η_{gear} is the gear box efficiency and λ_{gear} is the gear ratio. A static engine model is given by $Q_{\text{load}} = -\gamma_1 n_{\text{engine}} + \gamma_2$ with γ_1 and γ_2 being linearly dependent on fuel rate. A dynamic two-state model of the propeller is given by

$$2\pi I_{\text{prop}} \dot{n}_{\text{prop}} = Q_{\text{engine}} - Q_{\text{prop}} - n_{\text{friction}}$$
$$M_{\text{blade}} \dot{v}_{\text{prop}} = -D_{\text{blade}}(v_{\text{prop}} - v_{\text{f,ship}})|v_{\text{prop}} - v_{\text{f,ship}}| + T_{\text{prop}}$$

where I_{prop} is the propeller moment of inertia (including water added inertia), Q_{engine} is the torque produced by the engine, n_{friction} is the friction torque, M_{blade} is the added mass that is accelerated by the blades, and D_{blade} is a positive constant. This dynamic model can be used to replace the static relation $v_{\text{prop}} = v_{\text{f,ship}}(1-w)$. For a propeller acting in a tunnel (as is usually the case for thrusters used for positioning), $M_{\text{blade}} \approx \rho A L \gamma$ and $D_{\text{blade}} \approx \rho A \beta$ where A is the tunnel disc area, L is the tunnel length, γ is the effective added mass ratio, and β ($\sim$ 0.2-2) is the differential momentum flux coefficient across the propeller.

Control Surfaces (Rudders and Fins): The orientation of the control surface can be expressed in terms of the *central plane*, the long side of which is called the *span* and the short side the *chord*. The ratio of the mean span length to the mean chord length is called the *aspect ratio*. For large aspect ratios (> 3), the fluid flow can be considered as a two-dimensional problem and the forces generated by the action of the control surface can be obtained from the relative velocity component in the plane perpendicular to the span. For smaller aspect ratios, three-dimensional effects at the ends of the control surface become prominent also leading to increased drag. Denote by c_{cs} the unit vector along the chord and by n_{cs} the unit vector normal to the central plane. The unit vector along the span is given by $c_{\text{cs}} \times n_{\text{cs}}$. The effective force due to the control surface acts at the *center of pressure* r_{CP} whose location depends on the geometry of the control surface. Typically, the center of pressure is on the central plane around 60-75% out along the chord from the side of incoming flow and roughly midway along the span. The relative velocity of the center of pressure with respect to the surrounding water is given in the body-fixed frame by

$$v_{\text{rel}} = \dot{r}_{\text{CP}} + S(v_r) r_{\text{CP}} + R_i^{b\,T} [\dot{p}_t - v_{\text{water,CP}}] \qquad (35)$$

where $v_{\text{water,CP}}$ is the velocity of the water near the center of pressure expressed in the inertial frame[3]. The term $\dot{r}_{\text{CP}}$ in (35) which is the velocity of the center of pressure as seen in the body-fixed frame is zero if the control surface is fixed. If the orientation of the control surface relative to the ship is variable (as in the case of the rudder), this change in orientation influences the terms involving r_{CP} and $\dot{r}_{\text{CP}}$ in (35). The dynamics of the actuator (a simple model for rudder actuators being a rate and magnitude limited first-order integrator) used to move the control surface relative to the ship can be incorporated into the overall system dynamics.

[3]If the control surface is located close to the propeller, the relative velocity is influenced by the thruster action. This can be modeled by introducing a $v_{\text{water,CP}}$ with magnitude proportional to the square root of the thrust and with direction perpendicular to the heading.

The component v_{av} (the *advance velocity*) of the relative velocity in the plane perpendicular to the span is obtained by considering the components of v_{rel} in the normal and chord directions: $v_{\text{av}} = (v_{\text{rel}}^T n_{\text{cs}}) n_{\text{cs}} + (v_{\text{rel}}^T c_{\text{cs}}) c_{\text{cs}}$. The force due to the control surface depends on $|v_{\text{av}}| = \sqrt{(v_{\text{rel}}^T n_{\text{cs}})^2 + (v_{\text{rel}}^T c_{\text{cs}})^2}$ and on the *angle of attack* $\delta_{\text{attack}} = \text{atan2}(v_{\text{av}}.n_{\text{cs}}/|v_{\text{av}}|, v_{\text{av}}.c_{\text{cs}}/|v_{\text{av}}|)$, i.e., the angle between v_{av} and the chord. The control surface force can be decomposed into a *lift force* perpendicular to v_{av} and a *drag force* along v_{av}. Alternatively, the force can be decomposed into a *normal force* along n_{cs} and a *tangential force* along c_{cs}. Following the latter alternative, the normal and tangential forces are given by $F_{\text{N,cs}} = \frac{1}{2}\rho A_{\text{cs}} |v_{\text{av}}|^2 C_N(\delta_{\text{attack}})$ and $F_{\text{T,cs}} = \frac{1}{2}\rho A_{\text{cs}} |v_{\text{av}}|^2 C_T(\delta_{\text{attack}})$ where A_{cs} is the area of the projection of the control surface on the central plane. C_N and C_T are the normal and tangential force coefficients, respectively. For small δ_{attack}, C_N and C_T are proportional to δ_{attack}. C_N and C_T are monotonically increasing for $|\delta_{\text{attack}}| < \delta_{\text{stall}}$ where δ_{stall} is the *stall angle* and constant for $|\delta_{\text{attack}}| \geq \delta_{\text{stall}}$. A rough approximation for the dependence of the force coefficients on δ_{attack} is $C_N(\delta_{\text{attack}}) = C_{N0} \sin\left(\frac{\pi}{2} \frac{\delta_{\text{attack}}}{\delta_{\text{stall}}}\right)$ for $|\delta_{\text{attack}}| < \delta_{\text{stall}}$ and $C_N(\delta_{\text{attack}}) = C_{N0} \text{sign}(\delta_{\text{attack}})$ for $|\delta_{\text{attack}}| \geq \delta_{\text{stall}}$ with a similar model for C_T with C_{N0} replaced by C_{T0}. C_{N0} and C_{T0} are constant parameters depending on the control surface geometry. The generalized force vector due to the action of the control surface is

$$\overline{F}_{\text{cs}} = \frac{\rho A_{\text{cs}}}{2} |v_{\text{av}}|^2 \begin{bmatrix} C_N(\delta_{\text{attack}}) n_{\text{cs}} + C_T(\delta_{\text{attack}}) c_{\text{cs}} \\ r_{\text{CP}} \times [C_N(\delta_{\text{attack}}) n_{\text{cs}} + C_T(\delta_{\text{attack}}) c_{\text{cs}}] \end{bmatrix}.$$

The total force due to multiple control surfaces is obtained by adding the components due to the individual control surfaces.

IV. Controllers and Simulation Tests

We have developed a simulation package for testing the performance of controllers with the full six DOF model developed in this paper incorporating all the disturbance characterizations. A graphical visualization and interface environment (screenshot in Figure 1) has also been developed.

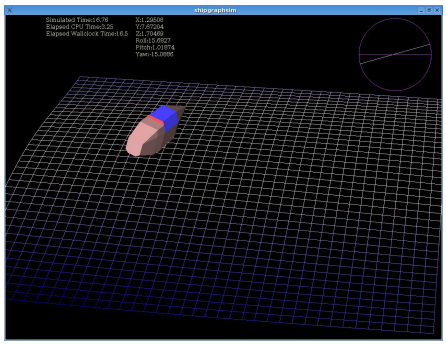

Fig. 1. Screenshot of USSV simulation package.

To highlight the importance of a six DOF modeling and to illustrate the impact of disturbances, simulations with two controllers are presented in this section. The first controller [11] is based on tracking of a reference trajectory generated by a nominal planar dynamics. The second controller is also based on the planar subsystem, but is designed via backstepping using the yaw reference as an intermediate control variable rather than an a priori provided reference trajectory. Given a planar reference trajectory $(x_{\text{ref}}, y_{\text{ref}})$, the backstepping-based controller is given by

$$z_1 = \dot{x}_{\text{ref}} - k_{x,p}(x - x_{\text{ref}}) - k_{x,i} \int_0^t (x - x_{\text{ref}}) d\tau \qquad (36)$$

$$z_2 = \dot{y}_{\text{ref}} - k_{x,p}(y - y_{\text{ref}}) - k_{x,i} \int_0^t (y - y_{\text{ref}}) d\tau \qquad (37)$$

$$\theta_{z,\text{ref}} = \text{atan2}(z_1, z_2)\ ,\ v_{t,x,\text{ref}} = \frac{z_1}{\cos(\theta_{z,\text{ref}})} = \frac{z_2}{\sin(\theta_{z,\text{ref}})} \qquad (38)$$

$$F_T = -M_{H,22} v_{t,y} v_{r,z} + d_{x,1} v_{t,x,\text{ref}} + d_{x,2} |v_{t,x,\text{ref}}| v_{t,x,\text{ref}}$$

$$-k_{x,d}(v_{t,x} - v_{t,x,\text{ref}}) + M_{H,11}\dot{v}_{t,x,\text{ref}} \quad (39)$$

$$\tau_R = -(M_{H,11} - M_{H,22})v_{t,x}v_{t,y} + d_{\theta_z,1}v_{r,z,\text{ref}} + d_{\theta_z,2}|v_{r,z,\text{ref}}|v_{r,z,\text{ref}} - k_{\theta_z,p}(\theta_z - \theta_{z,\text{ref}}) - k_{\theta_z,d}(\dot{\theta}_z - \dot{\theta}_{z,\text{ref}}) + M_{H,66}\ddot{\theta}_{z,\text{ref}} \quad (40)$$

where $k_{x,p}$, $k_{x,i}$, $k_{x,d}$, $k_{\theta_z,p}$, and $k_{\theta_z,d}$ are control gains.

A wave of frequency 1 rad/s, height 2.5 m (high end of sea state 4), and at direction 1.2 rad to the X-axis is introduced. The control objective is to track a straightline along the X-axis at 8 m/s. It is seen from Figure 2 that the first controller is not able to attenuate the sway disturbance and the Y error grows with time. The maximum X and Y errors in the 100 seconds of simulation are 5.3 m and 121.8 m, respectively. The maximum roll and pitch are 0.09 rad and 0.16 rad, respectively. In Figure 3, it is seen that the backstepping-based controller performs better and the sway tracking is significantly improved (maximum Y error of 20.3 m, RMS Y error of 9 m, and mean Y error of 5.9 m). The roll and pitch performance of the two controllers is comparable.

The controller of [11] is more sensitive to environmental disturbances that affect the sway since the yaw controller utilizes as yaw reference a signal generated *a priori* using the nominal planar dynamics. The approach in the backstepping-based controller is to provide robustness to such disturbances by generating the yaw reference online using the planar tracking errors. This corresponds to the physical observation that an intrinsic part of the steering policy would be to use the rudder to move towards the desired (x, y) location. This approach would also tend to turn the ship so that it faces oncoming waves since the wave-induced forces would tend to translate the ship along its direction of propagation. This would have the effect of attenuating roll motions due to waves.

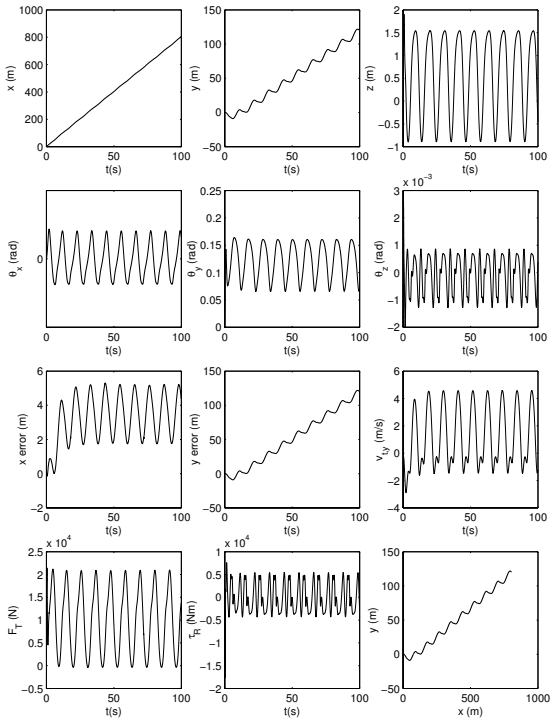

Fig. 2. Simulation results with controller of [11]: wave of frequency 1 rad/s, height 2.5 m, and angle 1.2 rad; forward speed 8 m/s.

It is expected that a controller that explicitly takes into account the form of the roll, pitch, and heave dynamics and the form of the disturbance forces and moments would be able to further improve the performance compared to controllers derived based purely on the planar subsystem. The detailed mathematical modeling presented in this paper is intended to provide the appropriate framework for such a control design which explicitly addresses the six DOF dynamics of the USSV along with the disturbances. Controllers specifically designed to attenuate six DOF wave-induced disturbances form the topic of ongoing research.

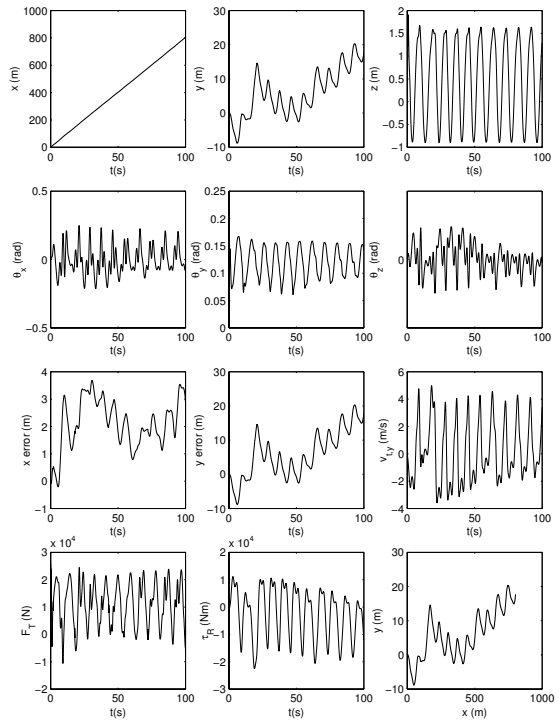

Fig. 3. Simulation results with backstepping-based controller : wave of frequency 1 rad/s, height 2.5 m, and angle 1.2 rad; forward speed 8 m/s.

REFERENCES

[1] J. N. Newman, *Marine Hydrodynamics*. Cambridge: The MIT Press, 1977.

[2] R. Bhattacharya, *Dynamics of Marine Vehicles*. New York: John Wiley and Sons, 1978.

[3] T. I. Fossen, *Guidance and Control of Ocean Vehicles*. New York: John Wiley and Sons, 1994.

[4] J. Goclowski and A. Gelb, "Dynamics of an automatic ship steering system," *IEEE Trans. on Automatic Control*, vol. 11, no. 3, pp. 513–524, July 1966.

[5] M. R. Katebi, M. J. Grimble, and Y. Zhang, "H_∞ robust control design for dynamic ship positioning," *IEE Proceedings - Control Theory and Applications*, vol. 144, no. 2, pp. 110–120, Mar. 1997.

[6] T. I. Fossen and A. Grovlen, "Nonlinear output feedback control of dynamically positioned ships using vectorial observer backstepping," *IEEE Trans. on Control Systems Technology*, vol. 6, no. 1, pp. 121–128, Jan. 1998.

[7] A. Loria, T. I. Fossen, and E. Panteley, "A separation principle for dynamic positioning of ships: theoretical and experimental results," *IEEE Trans. on Control Systems Technology*, vol. 8, no. 2, pp. 332–343, Mar. 2000.

[8] Y. Fang, E. Zergeroglu, M. S. de Queiroz, and D. M. Dawson, "Global output feedback control of dynamically positioned surface vessels: an adaptive control approach," in *Proceedings of the American Control Conference*, Arlington, VA, June 2001, pp. 3109–3114.

[9] F. Mazenc, K. Pettersen, and H. Nijmeijer, "Global uniform asymptotic stabilization of an underactuated surface vessel," *IEEE Trans. on Automatic Control*, vol. 47, no. 10, pp. 1759–1762, Oct. 2002.

[10] K. D. Do, Z. P. Jiang, and J. Pan, "Underactuated ship global tracking under relaxed conditions," *IEEE Trans. on Automatic Control*, vol. 47, no. 9, pp. 1529–1536, Sep. 2002.

[11] E. Lefeber, K. Y. Petterson, and H. Nijmeijer, "Tracking control of an underactuated ship," *IEEE Transactions on Control Systems Technology*, vol. 11, no. 1, pp. 52–61, Jan. 2003.

[12] Z. P. Jiang, A. Teel, and L. Praly, "Small-gain theorem for ISS systems and applications," *Mathematics of Control, Signals and Systems*, vol. 7, pp. 95–120, 1994.